8680 *Biochemistry* **2010,** *49,* 8680–8688
DOI: 10.1021/bi1009166

BIOCHEMISTRY
including biophysical chemistry & molecular biology
Article

tRNA Binding Properties of Eukaryotic Translation Initiation Factor 2 from *Encephalitozoon cuniculi*†

Marie Naveau, Christine Lazennec-Schurdevin, Michel Panvert, Yves Mechulam, and Emmanuelle Schmitt*

Ecole Polytechnique, Laboratoire de Biochimie, F-91128 Palaiseau Cedex, France, and CNRS, UMR7654, Laboratoire de Biochimie, Ecole Polytechnique, F-91128 Palaiseau Cedex, France

Received June 8, 2010; Revised Manuscript Received September 1, 2010

ABSTRACT: A critical consequence of the initiation of translation is the setting of the reading frame for mRNA decoding. In eukaryotic and archaeal cells, heterotrimeric initiation factor e/aIF2, in its GTP form, specifically binds Met-tRNA$_i^{Met}$ throughout the translation initiation process. After start codon recognition, the factor, in its GDP-bound form, loses affinity for Met-tRNA$_i^{Met}$ and eventually dissociates from the initiation complex. The role of each aIF2 subunit in tRNA binding has been extensively studied in archaeal systems. The isolated archaeal γ subunit is able to bind tRNA, but the α subunit is required for strong binding. Until now, difficulties during purification have hampered the study of the role of each of the three subunits of eukaryotic eIF2 in specific binding of the initiator tRNA. Here, we have produced the three subunits of eIF2 from *Encephalitozoon cuniculi*, isolated or assembled into heterodimers or into the full heterotrimer. Using assays following protection of Met-tRNA$_i^{Met}$ against deacylation, we show that the eukaryotic γ subunit is able to bind by itself the initiator tRNA. However, the two peripheral α and β subunits are required for strong binding and contribute equally to tRNA binding affinity. The core domains of α and β probably act indirectly by stabilizing the tRNA binding site on the γ subunit. These results, together with those previously obtained with archaeal aIF2 and yeast eIF2, show species-specific distributions of the roles of the peripheral subunits of e/aIF2 in tRNA binding.

Initiation of the translation of a messenger RNA into a protein involves a complex cascade of molecular events, leading to a translation-competent ribosome with a methionylated initiator tRNA in the P site, base-paired with the start codon on mRNA (*1*). A critical consequence of the whole process is the setting of the reading frame for mRNA decoding. In eukaryotic and archaeal cells, the initiator tRNA carrier is the e/aIF2 heterotrimer. In its GTP-bound form, this factor specifically binds Met-tRNA$_i^{Met}$ throughout the translation initiation process. After start codon recognition, the factor, in its GDP-bound form, loses affinity for Met-tRNA$_i^{Met}$ and eventually dissociates from the initiation complex. This leaves Met-tRNA$_i^{Met}$ in the P site of the small ribosomal subunit and allows the final steps of initiation to occur. In this process, specific binding of the initiator tRNA by e/aIF2 is crucial for accuracy. In both archaea and eukaryotes, Met-tRNA$_i^{Met}$ K_d values for full e/aIF2 heterotrimers are in the nanomolar range (*2*−*6*). However, how e/aIF2 binds initiator tRNA is still not fully understood.

e/aIF2 results from the association of three subunits, α, β, and γ. The γ subunit forms the core of the heterotrimer. It interacts with both the α and β subunits, while α and β do not interact with each other (*7*). Moreover, the structural resemblance of the γ subunit with EF-Tu, as well as site-directed mutagenesis studies, argues in favor of a binding mode of the tRNA molecule similar to that observed with the elongation factor (*2*, *6*−*9*).

By using archaeal aIF2, it was shown that the isolated γ subunit is indeed able to bind methionylated initiator tRNA. The measured tRNA binding affinity for aIF2γ is, however, greatly reduced compared to that obtained with the complete aIF2 heterotrimer. Indeed, the α subunit provides the heterotrimer with almost its full tRNA binding affinity, whereas the β subunit only slightly contributes to tRNA binding (*4*−*6*).

Because of difficulties during purification, the K_d value of Met-tRNA$_i^{Met}$ for an isolated eukaryotic γ subunit has never been measured and the roles of eIF2α and eIF2β subunits in tRNA binding have been controversial for many years (*10*). However, the construction of a yeast strain completely lacking eIF2α, allowing purification of an eIF2$\beta\gamma$ heterodimer, has shown that α contributes only slightly to tRNA binding affinity (a factor of no more than 5) (*11*). In contrast, β appears to have an important role in tRNA binding (*12*). Therefore, a "eukaryotic behavior", with a major role for the β subunit in the binding of the tRNA and a minor role for the α subunit, would be opposed to an "archaeal behavior" in which α makes the major contribution. In this view, eIF2 forms from other species need to be studied to further evaluate the participation of the peripheral subunits in tRNA binding.

Microsporidia are unicellular eukaryotes living as obligate intracellular parasites. The genome of *Encephalitozoon cuniculi* has been sequenced (*13*). Consisting of 11 linear chromosomes, the *E. cuniculi* genome is remarkably small (~2.9 Mb). Because the genome contains genes related to some mitochondrial functions, microsporidia are thought to have retained a mitochondrion-derived organelle called the mitosome (*13*). Phylogenetic analysis supports the proximity of microsporidia with fungi even though the question of whether microsporidia are true fungi or only related to fungi is still debated (*14*−*16*).

†This work was supported in part by the ANR (PCV-MASTIC). M.N. was a recipient of a Gaspard Monge Ph.D. scholarship from Ecole Polytechnique.

*To whom correspondence should be addressed: Laboratoire de Biochimie, Ecole Polytechnique, F-91128 Palaiseau cedex, France. Telephone: +33 1 69334885. Fax: +33 1 69334909. E-mail: emma@botrytis.polytechnique.fr.

 Published on Web 09/07/2010

In this study, we were able for the first time to produce and purify the three subunits of a eukaryotic eIF2 complex, that from *E. cuniculi* (Encc-eIF2).[1] The subunits were produced isolated or assembled into heterodimers or into the full heterotrimer. Using assays following protection of Met-tRNA$_i^{Met}$ against deacylation, constants for dissociation of Met-tRNA$_i^{Met}$ from various eIF2−Gpp(NH)p−Met-tRNA$_i^{Met}$ complexes were measured. This allowed us to establish that, like its archaeal counterpart, the eukaryotic γ subunit by itself is able to bind Met-tRNA$_i^{Met}$. Unexpectedly, in contrast with both the yeast and archaeal cases, α and β contribute comparably to tRNA binding affinity for the Encc-eIF2 heterotrimer. The peripheral subunits probably act indirectly on tRNA binding by stabilizing the two switch regions in the G domain of the γ subunit. Hence, we propose that the species-specific distribution of the roles of the peripheral subunits of e/aIF2 originates from modulation of the interactions at the interfaces between α and γ or between β and γ.

EXPERIMENTAL PROCEDURES

Cloning and Expression of eIF2 Subunits from E. cuniculi. The genes encoding the α, β, and γ subunits of eIF2 were amplified by polymerase chain reaction (PCR) from *E. cuniculi* DNA (generous gift from F. Delbac, Aubière, France) and cloned in pET derivative vectors. The gene encoding the α subunit was cloned between the NcoI and SacII restriction sites of a modified version of pET15b, pET15blpa (*17*). The resulting plasmid, pET15blpaα-Encc, led to the expression of an untagged α subunit of *E. cuniculi* in *Escherichia coli*. The gene encoding the β subunit was cloned between the NdeI and SacII restriction sites of pET15blpa to give pET15blpaβtn-Encc. The resulting protein carries a six-histidine tag at its N-terminus. Finally, the gene encoding the γ subunit was cloned into the NcoI and SacII restriction sites of pET28b+ (Merck, Novagen) to give pET28b+ γtc-Encc. The resulting protein carries a six-histidine tag at its C-terminus, preceded by a thrombin cut site.

Each subunit was overexpressed separately. Each vector was introduced into *E. coli* BL21 Rosetta pLacI-Rare (Merck, Novagen). Cultures (1 L) were in 2×TY containing 50 μg/mL ampicillin and 34 μg/mL chloramphenicol. For β and γ subunits, expression was induced via addition of 1 mM IPTG when OD_{650} reached 0.8. For the α subunit, expression was induced after an overnight culture at 37 °C ($OD_{650} \sim 2.5$) via addition of 1 mM IPTG. After induction, the cultures were continued for 8−12 h at 18 °C.

Purification of Encc-eIF2γ. Overproducing cells corresponding to 1 L of culture were disrupted by sonication in 30 mL of buffer A [10 mM HEPES (pH 7.5), 500 mM NaCl, 3 mM 2-mercaptoethanol, 0.1 mM PMSF, and 0.1 mM benzamidine]. The crude extract was recovered after centrifugation and loaded onto a Q-Sepharose column [16 mm × 20 cm (GE-Healthcare)] equilibrated in buffer A. This step allowed removal of most of the nucleic acids. The protein was recovered in the flow-through fraction (FT) and then loaded onto a column (1 mL) containing Talon affinity resin (Clontech) equilibrated in buffer A. The resin was first washed with 10 mL of buffer A and then with 10 mL of buffer A supplemented with 10 mM imidazole. Finally, the protein was eluted with buffer A containing 125 mM imidazole. The recovered protein was then diluted to 150 mM NaCl and successively passed through an S-Hiload column and a Q-Hiload column equilibrated in buffer B [10 mM HEPES (pH 7.5), 150 mM NaCl, 3 mM 2-mercaptoethanol, 0.1 mM PMSF, and 0.1 mM benzamidine]. Finally, to polish the preparation, the protein was loaded onto a Superdex 75 column (HR 10/30, GE Healthcare) equilibrated in buffer C [10 mM HEPES (pH 7.5), 300 mM NaCl, 3 mM 2-mercaptoethanol, 0.1 mM PMSF, and 0.1 mM benzamidine]. Fractions containing Encc-eIF2γ were pooled and concentrated by using a Centricon 30 concentrator (Amicon). Either 1 mM Gpp(NH)p-Mg^{2+} or 1 mM GDP-Mg^{2+} was added before storage of the protein at 4 °C. Approximately 1.5 mg of Encc-eIF2γ was purified from 1 L of culture.

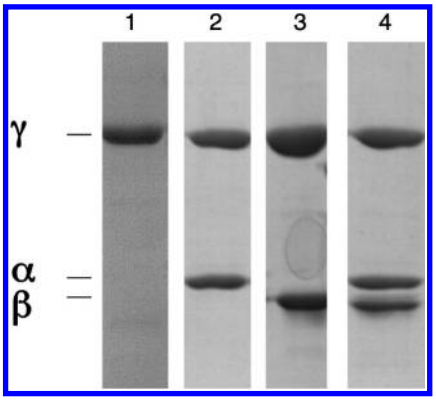

FIGURE 1: SDS−PAGE analysis of Encc-eIF2. The 12.5% SDS−polyacrylamide gel was stained with Coomassie Blue: lane 1, Encc-eIF2γ; lane 2, Encc-eIF2αγ heterodimer; lane 3, Encc-eIF2αβ heterodimer; lane 4, Encc-eIF2 heterotrimer. The positions of Encc-eIF2α (32.1 kDa), N-terminally tagged-Encc-eIF2β (28.1 kDa), and C-terminally tagged-Encc-eIF2γ (48.9 kDa) are indicated. Purifications were performed as described in Experimental Procedures.

Purifications of Encc-eIF2αβγ, -βγ, and -αγ Complexes. (*i*) *Purification of Encc-eIF2αβγ.* Cultures of cells overproducing each of the three subunits (500 mL for α, 500 mL for γ, and 1 L for β) were harvested, mixed in 80 mL of buffer A, and disrupted by sonication. After centrifugation, the supernatant was loaded onto a Q-Sepharose [16 mm × 20 cm (GE-Healthcare)] column equilibrated in buffer A. The protein was recovered in the FT fraction and then loaded onto a column (3 mL) containing Talon affinity resin (Clontech) equilibrated in the same buffer. The resin was first washed with 10 mL of buffer A and then with 10 mL of buffer A supplemented with 10 mM imidazole. The fractions containing the heterotrimer were finally recovered after elution with buffer A containing 125 mM imidazole. Because both β and γ subunits carried a histidine tag, a supplementary step was performed to achieve the correct stoichiometry among the three subunits. The affinity column eluate was diluted to 150 mM NaCl and then loaded on an S-Hiload column equilibrated in buffer B [10 mm × 5 cm (GE Healthcare)]. A gradient from 150 to 600 mM NaCl was used for elution (120 mL at a flow rate of 2 mL/min). After SDS−PAGE analysis, the fractions containing the heterotrimer were pooled and dialyzed against buffer C. Finally, the protein was concentrated by using Centricon 30 concentrators. Either 1 mM Gpp(NH)p-Mg^{2+} or 1 mM GDP-Mg^{2+} was added before storage at 4 °C of the recovered heterotrimer. Routinely, ~500 μg of purified heterotrimer was obtained.

(*ii*) *Purification of Encc-eIF2αγ and -βγ Heterodimers.* The same procedure that is described above for the purification of the complete eIF2 heterotrimer was used to purify the two heterodimers, Encc-eIF2αγ and Encc-eIF2$\beta\gamma$. An SDS−PAGE

[1]Abbreviations: Encc-eIF2, eIF2 from *E. cuniculi*; Ss-aIF2, aIF2 from *Sulfolobus solfataricus*; Pa-aIF2, aIF2 from *Pyrococcus abyssi*; Pf-aIF2, aIF2 from *Pyrococcus furiosus*.

analysis of the purified proteins is shown in Figure 1. After purification, the heterodimers were dialyzed against buffer C and further concentrated by using Centricon 30 concentrators. Either 1 mM Gpp(NH)p-Mg^{2+} or 1 mM GDP-Mg^{2+} was added before storage of the recovered protein at 4 °C. Routinely, ~500 μg of purified heterodimers was obtained.

(*iii*) *Production of Mutant Proteins*. Deletions in the target genes were conducted according to the QuikChange site-directed mutagenesis method (Stratagen). The full sequence of all mutated genes was confirmed by resequencing. Deletion of the N-terminal domain of eIF2β was achieved using pET15blpaβtn-Encc to give pET15blpaβtnΔN-Encc. The construction led to the expression of a β subunit starting at residue I71 and carrying a six-histidine tag at its N-terminus. Deletion of the C-terminal domain of eIF2β was achieved using pET15blpaβtn-Encc to give pET15blpaβtnΔC-Encc. The construction led to the expression of a β subunit ending at residue A210 and carrying a six-histidine tag at its N-terminus. The doubly deleted mutant eIF2$\beta\Delta$NΔC was constructed using pET15blpaβtnΔN-Encc to give pET15blpaβtnΔNΔC-Encc. eIF2αD3 was constructed using pET15blpaα-Encc to give pET15blpaαD3-Encc. eIF2αD3 starts at residue A247 of the eIF2α sequence. Finally, deletion of the C-terminal domain of eIF2α was achieved using pET15blpaα-Encc to give pET15blpa$\alpha\Delta$C-Encc. The construction led to the expression of an α subunit ending at residue G263.

Protection Assay. $tRNA_f^{Met}$, $tRNA_1^{Val}$, and their variants were produced in *E. coli* from synthetic genes as described previously (*18*, *19*). The gene for $tRNA_i^{Met}$ from *E. cuniculi* was constructed by assembly of oligonucleotides and inserted into pBSTNAV2 (*20*). tRNAs were purified by anion exchange chromatography (*20*). Amino acid acceptor capacities were between 800 and 1400 pmol per A_{260} unit. Full aminoacylation with [^{35}S]methionine [ca. 10000 dpm/pmol (Perkin-Elmer)] was achieved using homogeneous *E. coli* M547 MetRS (*21*). Valylation with [^{3}H]Val [4500 dpm/pmol (Amersham)] was performed with homogeneous *E. coli* ValRS (*22*). Aminoacyl-tRNAs were precipitated with ethanol in the presence of 0.3 M NaAc (pH 5.5) and stored at −20 °C in 100% EtOH in small aliquots. Before use, aminoacylated tRNAs were redissolved in water and full aminoacylation was systematically controlled after precipitation in 5% TCA.

Protection by Encc-eIF2 of aminoacylated tRNAs against spontaneous hydrolysis (*23*) was performed as follows. Reaction mixtures (150 μL) contained 20 mM HEPES-NaOH (pH 8.0), 100 mM NaCl, 5 mM $MgCl_2$, 1 mM DTT, 0.1 mM EDTA, 0.2 mg/mL BSA [bovine serum albumin (Roche)], 5% glycerol, 0.1% Triton X-100, 1 mM GDPNP, and the aminoacylated tRNA under consideration (2 nM). Concentrations of Encc-eIF2 or its variants were varied from 1 nM to 3 μM according to the K_d value to be measured. The mixtures were incubated at 30 °C. To determine the rate constants of deacylation, 20 μL aliquots were withdrawn at various times (usually, six aliquots from 5 to 60 min) and precipitated in 5% TCA in the presence of 80 μg of yeast RNA as a carrier. In all cases, the deacylation curve as a function of time could be fitted with a single exponential. For each K_d measurement, a set of 8−10 experiments corresponding to 8−10 different protein concentrations was performed. The rate constants measured at variable protein concentrations were then fitted to simple binding curves from which the dissociation constant of the studied protein−tRNA complexes could be deduced using MC-Fit (*24*). For K_d values of < 10 nM, an aminoacylated tRNA concentration of 0.67 nM was used in reaction mixtures of 300 μL. In these cases, to determine the rate constants of deacylation, 40 μL aliquots were withdrawn at various times (from 5 to 60 min). Typical plots of the derived rate constants as a function of protein concentration are illustrated in Figure 3. The concentrations of the proteins were determined from A_{280} measurements using extinction coefficients computed from the amino acid sequences.

RESULTS

Production and Assembly of Encc-eIF2 Subunits. Blast sequence comparisons have allowed identification of the three genes encoding eIF2 subunits (ref *13* and this study). Each subunit of the heterotrimeric protein eIF2 from *E. cuniculi* (α, 32.1 kDa; β, 26 kDa; γ, 48 kDa) was produced independently in *E. coli* and purified. To facilitate purification, the γ subunit was produced with a six-histidine tag added to its C-terminal end and the β subunit was produced with a six-histidine tag added to its N-terminal end (see Experimental Procedures). The heterodimers ($\alpha\gamma$ and $\beta\gamma$) and the heterotrimer ($\alpha\beta\gamma$) were purified by mixing cell pellets corresponding to independent cultures of each isolated subunit before lysis. After affinity chromatography, anion exchange chromatography was performed to recover the stoichiometric complexes (Figure 1). These purifications showed that the γ subunit was able to interact with both the α and β subunits. In contrast, when cultures overproducing Encc-eIF2α and His-tagged Encc-eIF2β were mixed and sonicated, and the soluble proteins passed through Talon Ni-affinity resin, only the β subunit was retained on the resin. Therefore, as observed in the case of yeast eIF2 (*25*, *26*) or archaeal aIF2 subunits (*4*, *7*, *27*), α and β are bound to γ but do not interact with each other. The zinc contents of γ, $\alpha\gamma$, and $\alpha\beta\gamma$ were determined by atomic absorption spectroscopy (data not shown). Our results were consistent with β and γ proteins each containing one tightly bound zinc ion, in agreement with the conservation of zinc binding cysteine clusters in their respective sequences.

Binding of Initiator Met-tRNA to Encc-eIF2. Binding of $tRNA_i^{Met}$ to eIF2 leads to protection of aminoacylated tRNA against spontaneous deacylation. Thus, constants for dissociation of Met-$tRNA_i^{Met}$ from its complex with eIF2 can be estimated by following deacylation rates in the presence of various eIF2 concentrations at a fixed tRNA concentration (*6*, *23*). First, we overexpressed in *E. coli* a gene corresponding to the initiator tRNA of *E. cuniculi*. The product of this gene, $tRNA_i^{Met}$, was purified, aminoacylated with [^{35}S]methionine, and assayed for its ability to bind Encc-eIF2 in the presence of either 1 mM GTP-Mg^{2+} or 1 mM Gpp(NH)p-Mg^{2+}. In the presence of GTP, the measured K_d value was 4.3 ± 0.7 nM. In the presence of Gpp(NH)p, the K_d value was 3.8 ± 0.7 nM (Table 1, row 1). Moreover, in the presence of GDP instead of Gpp(NH)p, the K_d value was increased to 138 ± 50 nM. Therefore, Encc-eIF2 is able to bind efficiently its cognate methionylated initiator tRNA. The binding affinity, in the nanomolar range, is on the same order of magnitude as that measured for yeast eIF2 [9 nM (*3*)] or for aIF2 from *Sulfolobus solfataricus* (Ss-aIF2) [1.5 nM (*5*)]. Moreover, GDP lowered the binding affinity of the methionylated initiator tRNA by a factor of 36, in keeping with the nucleotide effects observed with yeast eIF2 [factor of 20 (*3*)] or Ss-aIF2 [factor of 100 (*5*)]. Because the K_d values were not significantly different in the presence of either GTP or Gpp(NH)p, we chose to use the nonhydrolyzable analogue in the following experiments, to avoid potential problems linked to nucleotide hydrolysis.

Table 1: Constants for Dissociation of Met-tRNA$_f^{Met}$ from Its Complexes with the Indicated Combinations of Wild-Type (wt) or Mutant eIF2 Subunits from *E. cuniculi*[a]

	α	β	γ	K_d (nM) in the presence of Gpp(NH)p	K_d (nM) in the presence of GDP
1	wt	wt	wt	3.8 ± 0.7[b]	138 ± 50[c]
2	wt	wt	wt	4.2 ± 0.3[d]	330 ± 100
3	−	−	wt	1700 ± 300	> 24000
4		wt	wt	22 ± 1	> 3000
5	wt	−	wt	18 ± 2	1000 ± 500
6	−	ΔN	wt	37 ± 2	> 3000
7	−	ΔC	wt	73 ± 6	> 3000
8		ΔNΔC	wt	71 ± 3	> 3000
9	ΔC	−	wt	23 ± 5	3000 ± 1000
10	D3		wt	87 ± 16	> 3000
11	D3	wt	wt	11 ± 2	> 3000

[a]The values shown are derived from plots of the deacylation rate as a function of the concentration of eIF2 variants. Values are means ± the standard deviation from at least two independent experiments. Protection experiments were performed at 30 °C. Unless otherwise stated, experiments were performed in the presence of 2 nM *E. coli* Met-tRNA$_f^{Met}$ and the indicated nucleotide at 1 mM. [b]Experiment performed in the presence of 0.67 nM *E. cuniculi* Met-tRNA$_i^{Met}$. [c]Experiment performed in the presence of 2 nM *E. cuniculi* Met-tRNA$_i^{Met}$. [d]Experiment performed in the presence of 0.67 nM *E. coli* Met-tRNA$_f^{Met}$.

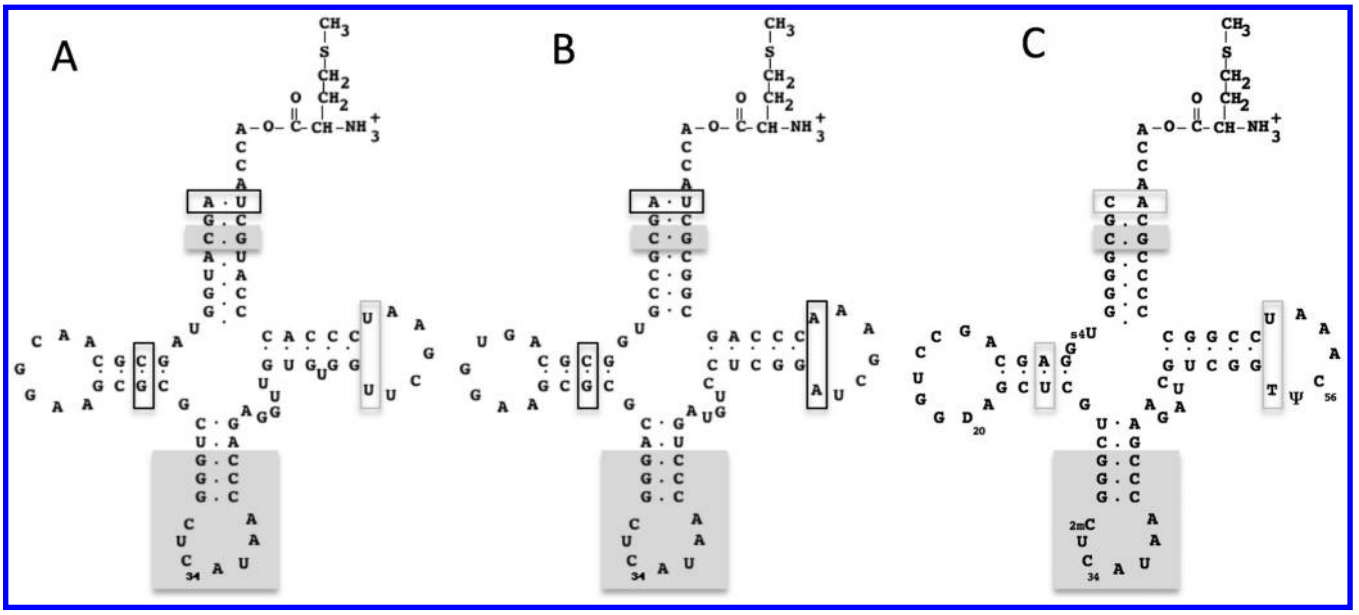

FIGURE 2: Coverleaf representations of initiator Met-tRNA^{Met}: (A) *E. cuniculi* Met-tRNA$_i^{Met}$, (B) yeast cytoplasmic Met-tRNA$_i^{Met}$, and (C) *E. coli* Met-tRNA$_f^{Met}$. Nucleotides denoted with gray boxes are universally conserved in initiator tRNA^{Met}. Nucleotides denoted with black lines are found in most eukaryotic and archaeal initiator tRNAs. Nucleotides denoted with gray lines are characteristic of bacterial initiator tRNA^{Met}.

E. cuniculi tRNA$_i^{Met}$ possesses all the identity elements of eukaryotic initiator tRNAs. The only exceptions are bases U54 and U60 in the T loop, characteristic of archaeal and bacterial initiator tRNAs (*28*) (Figure 2). Moreover, it was previously observed (*3*, *6*) that the highly conserved A1-U72 base pair of archaeal and eukaryal initiator tRNAs is not strictly required for e/aIF2 binding. Therefore, *E. coli* Met-tRNA$_f^{Met}$ initiator tRNA was tested as a ligand of Encc-eIF2. Indeed, *E. coli* Met-tRNA$_f^{Met}$ appeared to bind Encc-eIF2 as strongly as the *E. cuniculi* initiator tRNA produced in *E. coli* (Table 1, rows 1 and 2). This comparison shows that the change of an A1-U72 base pair into a C_1-A_{72} mismatch has no significant effect on binding to eIF2 in the *E. cuniculi* system. This result validated the use of *E. coli* Met-tRNA$_f^{Met}$ as a model ligand for the further study of formation of the complex between Encc-eIF2 and tRNA.

The specificity of tRNA binding to Encc-eIF2 was evaluated using several aminoacylated tRNAs (Table 2). First, the specificity of the factor toward the methionine moiety of the initiator Met-tRNA was studied by using a tRNA$_f^{Met}$ variant with the UAC anticodon instead of the CAU one. This variant can be aminoacylated with valine in the presence of *E. coli* ValRS (*18*, *29*). The K_d value of this valylated initiator tRNA was reduced by a factor 220, compared to that of Met-tRNA$_f^{Met}$ (Table 2, rows 2 and 6). On the other hand, two other tRNAs, distinct from the initiator tRNA but aminoacylated with methionine, were efficiently protected against deacylation (Table 2, rows 4 and 5). The first one was *E. coli* elongator Met-tRNA$_m^{Met}$. The second one was a derivative of tRNA$_1^{Val}$ carrying a CAU anticodon that allows its aminoacylation by MetRS (*29*). We therefore concluded that the methionyl moiety plays a crucial role in the binding to the factor. However, the dissociation constants of the two methionylated tRNAs described above were increased by a factor of 3, compared to that of Met-tRNA$_f^{Met}$. This difference indicates some influence of the tRNA sequence on

eIF2 binding. Notably, these two methionylated tRNAs possess a G1-C72 pair. Therefore, to test the role of the G1-C72 base pair in tRNA recognition by Encc-eIF2, an *E. coli* $tRNA_f^{Met}$ variant with a G1-C72 base pair instead of the wild-type unpaired C1 and A72 bases was prepared. Encc-eIF2 protected this Met-tRNA against deacylation. However, the dissociation constant of this ligand was increased by a factor of 2.6 compared to that of authentic Met-$tRNA_f^{Met}$ (Table 1, rows 2 and 3). Hence, we conclude that the absence of strong base pairing at positions 1 and 72 as in *E. cuniculi* $tRNA_i^{Met}$ or in *E. coli* $tRNA_f^{Met}$ contributes to the optimal binding to Encc-eIF2. These results are fully consistent with those previously obtained using yeast eIF2 and Pa-aIF2 (*3*, *6*).

Table 2: Constants for Dissociation of Aminoacylated tRNAs from Their Complexes with Wild-Type Encc-eIF2[a]

	tRNA variant	K_d (nM)
1	*E. cuniculi* Met-$tRNA_i^{Met}$	3.8 ± 0.7
2	Met-$tRNA_f^{Met}$	4.2 ± 0.3
3	Met-$tRNA_f^{Met}$ G1-C72	11 ± 3
4	Met-$tRNA_m^{Met}$	14 ± 2
5	Met-$tRNA_1^{Val}$ CAU	13 ± 3
6	Val-$tRNA_f^{Met}$ UAC	930 ± 180

[a]The values are derived from the plot of the deacylation rates as a function of the concentration of eIF2 measured at 30 °C in the presence of a fixed aminoacyl-tRNA concentration (0.67 nM for all tRNAs with the exception of Val-$tRNA_f^{Met}$ UAC, for which a concentration of 1 μM was used) and 1 mM GDPNP (see Experimental Procedures). Values are means ± the standard deviation from at least two independent experiments.

Both α and β Subunits Are Required for Optimal Binding of tRNA to Encc-eIF2. Biochemical and structural data suggest a pivotal role of the γ subunit in the binding of tRNA (*2*, *5*−*7*, *30*). Until now, the isolated γ subunit of Pa-aIF2 was shown to be able to bind Met-$tRNA_i^{Met}$ [K_d = 5 μM (*6*)]. Using the isolated γ subunit of Ss-aIF2, the K_d value was not measurable (*5*). However, significant protection against spontaneous deacylation was observed at 51 °C using a concentration of Ss-aIF2γ of 100 μM. The deacylation rate was 0.09 ± 0.005 min^{-1}, a value significantly smaller than the rate of spontaneous deacylation (0.13 ± 0.005 min^{-1}). Such protection was not observed in the presence of GDP. Therefore, weak but significant

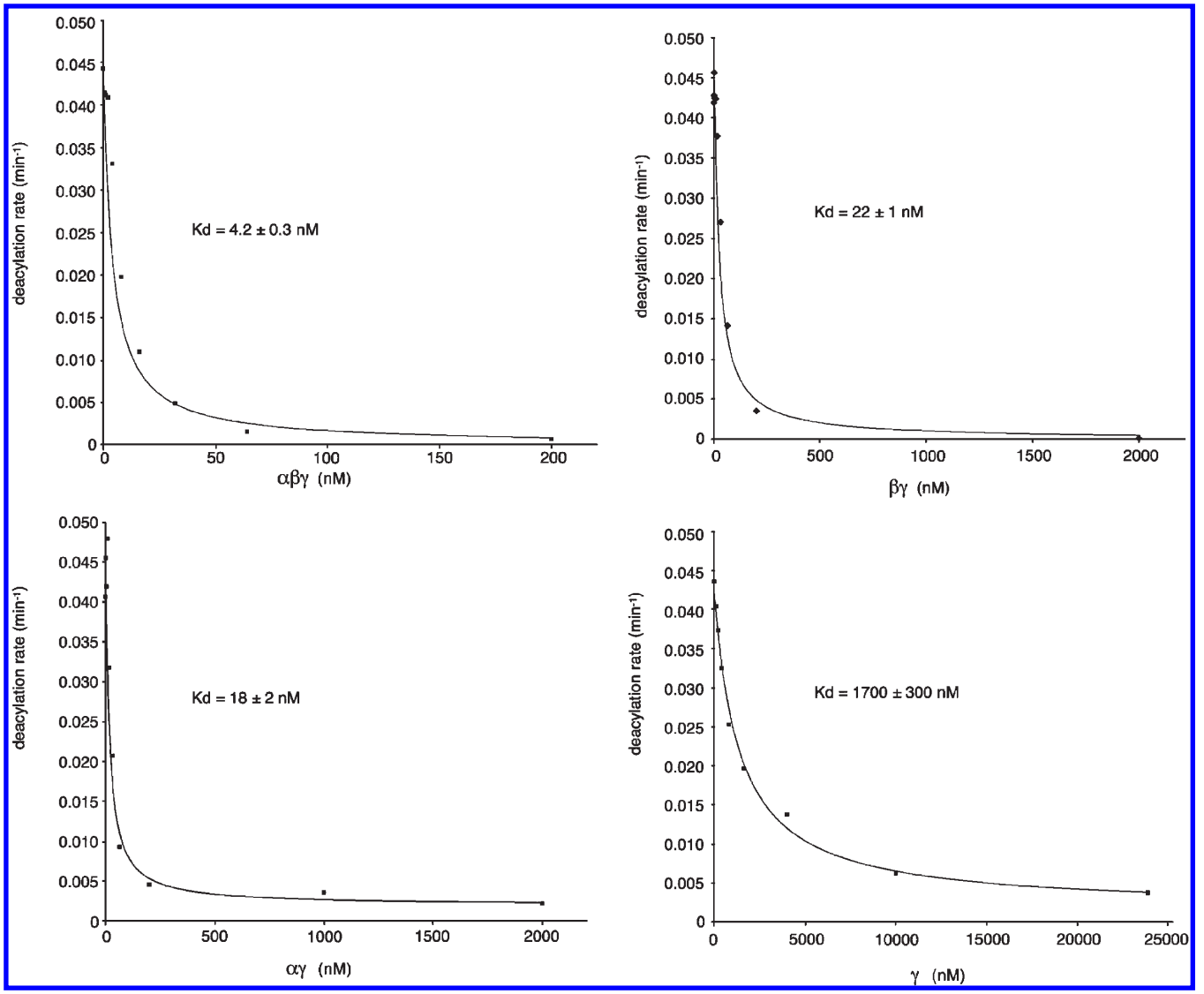

FIGURE 3: tRNA binding by Encc-eIF2 and its subcomplexes. Plots of the measured deacylation rate constants as a function of protein concentration are shown. Each rate constant was derived from the fit of a single exponential to a deacylation curve defined by six experimental points. From the binding curve, a constant for dissociation of the Met-$tRNA_f^{Met}$ from its complex was derived.

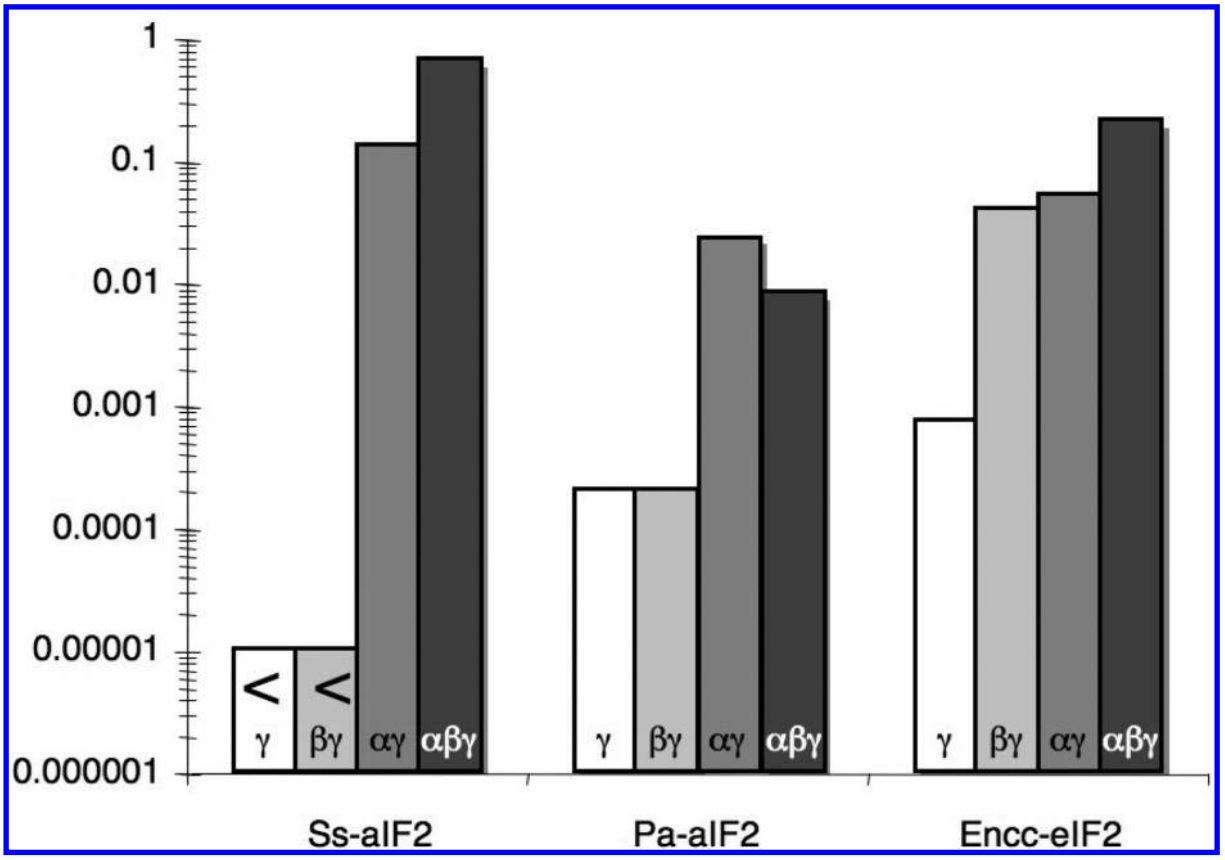

FIGURE 4: Graphical representation of the affinity constants of Met-tRNA$_i^{Met}$ from their complexes with the indicated e/aIF2 derivatives. The vertical axis is logarithmically scaled. Ss-aIF2 stands for aIF2 from *S. solfataricus*. Results are from this study and ref *5*. The < sign means that the K_a values are lower than the values indicated by the tops of the bars. Pa-aIF2 stands for aIF2 from *Pyrococcus abyssi* (*6*).

Gpp(NH)p-dependent binding of initiator tRNA to Ss-aIF2γ also occurred.

Because of difficulties during purification, binding of tRNA to the isolated γ subunit of a eukaryotic eIF2 has never been studied. Here, we successfully produced and purified Encc-eIF2γ, and we could therefore evaluate its tRNA binding capacity. As shown in Table 1 and Figure 3, the isolated γ subunit of *E. cuniculi* is active in the Gpp(NH)p-dependent protection against deacylation, although the corresponding dissociation constant is 400 times higher than that measured with the complete heterotrimer (Table 1, rows 2 and 3). Therefore, like its archaeal counterparts, Encc-eIF2γ is able to bind methionylated initiator tRNA in a GTP-dependent manner.

The large difference between the K_d value with the γ subunit and that with the full eIF2 trimer suggests that the α and/or the β subunit participates in tRNA binding. To test this idea, Met-tRNA$_f^{Met}$ dissociation constants were measured with either the $\alpha\gamma$ or $\beta\gamma$ heterodimer (Table 1, rows 4 and 5, and Figure 3). Using $\beta\gamma$, the K_d value of Met-tRNA$_i^{Met}$ was 22 $\pm$ 1 nM. Therefore, the β subunit improves the binding affinity of Met-tRNA$_i^{Met}$ for the γ subunit by a factor of 77 (Table 1, rows 3 and 4). It should be underlined that, in the absence of the α subunit, the K_d value for Met-tRNA$_f^{Met}$ is lowered by a factor of only 5, compared to that measured with the full heterotrimer. However, a K_d value of 18 $\pm$ 2 nM was measured for Met-tRNA$_f^{Met}$ binding to $\alpha\gamma$. Therefore, the α subunit improves the binding affinity of Met-tRNA$_f^{Met}$ for the γ subunit by a factor of 94 (Table 1, rows 3 and 5). Again, in the absence of the β subunit, the K_d value for Met-tRNA$_f^{Met}$ is lowered by a factor of only 4, compared to that measured with the full heterotrimer. Hence, on one hand, the α and β subunits both participate in the binding of tRNA to Encc-eIF2. Their respective contributions are important and on the same order of magnitude (Figure 4). On the other hand, the contributions of α and β subunits to the affinity of Met-tRNA$_f^{Met}$ for Encc-eIF2 are not additive, indicating that these contributions are not independent.

In archaea, the isolated C domain of aIF2α, αD3, responsible for binding to γ, is enough to confer on the γ subunit the same binding affinity for tRNA as full aIF2 (*5*, *6*). The C-terminal domain of Encc-eIF2α (αD3) was produced and purified. This domain was able to bind Encc-eIF2γ and to largely stimulate tRNA binding. The tRNA binding affinity for the αD3γ dimer is reduced by a factor of 4.8 compared to that measured for $\alpha\gamma$ (Table 1, rows 5 and 10). With αD3$\beta\gamma$, the tRNA binding affinity is reduced by a factor of only 2.6 compared to that measured for the wild-type $\alpha\beta\gamma$ heterotrimer. These results show that αD3 accounts for most of the effect of the α subunit on tRNA binding. However, the minor participation of the rest of α (αD12 domains) cannot be excluded. Notably, the presence of β at least partly compensates for the absence of αD12 (Table 1, rows 11 and 2). This is consistent with the effects of α and β on tRNA binding being nonindependent.

Extensions of Encc-eIF2α and -β Are Not Essential for tRNA Binding. To identify a possible origin for the different behaviors observed between the various species of e/aIF2, the structural organization of the α, β, and γ subunits was compared. Sequence alignments were performed for the three subunits (Figures S1−S3 of the Supporting Information). The α, β, and γ subunits contain a conserved structural core corresponding to the archaeal version of the subunits, whereas eukaryotic versions contain species-specific N- and C-terminal extensions (Figure 5).

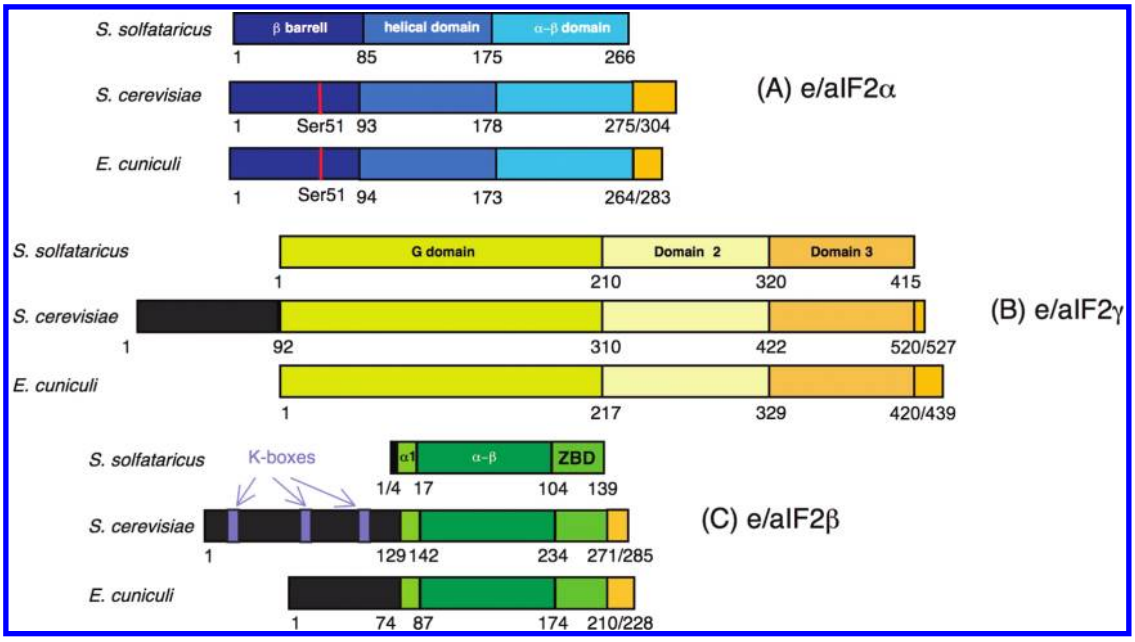

FIGURE 5: Schematic structural organization of initiation factors based on alignments of eukaryotic and archaeal initiation factors. The structural organization of the initiation factor from *E. cuniculi* was compared to that of the corresponding factor in *Saccharomyces cerevisiae* and in *S. solfataricus*. The colored boxes indicate regions of significant sequence similarity between the proteins. The numbering refers to the limits of characterized structural domains in each species. The scheme is to scale. In panel A, 142 e/aIF2α sequences were aligned; the C-terminal extension to the core domain of e/aIF2α is shown as an orange box. In panel B, 108 e/aIF2γ sequences were aligned; the N-terminal extension to the core domain of e/aIF2γ is shown as a brown box, and the C-terminal extension is shown as an orange box. In panel C, 142 e/aIF2β sequences were aligned; the N-terminal extension to the core domain of e/aIF2β is shown as a brown box, and the C-terminal extension is shown as an orange box.

Within the conserved structural cores of the three subunits, these alignments have allowed us to highlight some positions specific to the archaeal domain of life and some positions specific to the eukaryotic domain of life (Figures S1−S3 of the Supporting Information). The sequences of the three subunits of Encc-eIF2 were then compared to these two resulting patterns. Clearly, the cores of the three subunits of Encc-eIF2 are of the eukaryotic type (Figures S1−S3 of the Supporting Information). In contrast, as shown in Figure 5, Encc-eIF2 subunits possess shorter N- and C-terminal extensions compared to those of yeast eIF2 subunits. The only exception is the C-terminal extension of Encc-eIF2β that is four residues longer than that present in yeast eIF2β.

To evaluate the roles of the basic N- and C-terminal extensions of Encc-β, truncated versions of the subunit were produced. In βΔN, the first 69 residues were removed. Notably, although this N-terminal extension is basic in character, it does not contain the three lysine boxes found in other eukaryotic eIF2β forms. In βΔC, the last 18 residues were removed. The double mutant βΔNΔC was also constructed. The corresponding modified βγ heterodimers were purified and tested for their abilities to bind Met-tRNA$_i^{Met}$. The C-terminal extension of Encc-eIF2β contributed by a factor of 3.3 to the tRNA binding affinity for a βγ heterodimer (Table 1, rows 4 and 7). The N-terminal extension of Encc-eIF2β contributes only weakly to the tRNA binding affinity for a βγ heterodimer [factor of 1.7 (Table 1, rows 4, 6, and 8)].

A truncated mutant of eIF2α, αΔC, was constructed via removal of the last 19 residues, which constitute an acidic C-terminal extension. As shown in Table 1 (rows 5 and 9), removal of this extension had no significant effect on tRNA binding to an αγ heterodimer.

DISCUSSION

In this study, the three subunits of Encc-eIF2 were produced separately and used to reconstitute αγ and βγ heterodimers as well as the full αβγ heterotrimer. Using assays following protection of Met-tRNA$_i^{Met}$ against deacylation, constants for dissociation of Met-tRNA$_i^{Met}$ from various eIF2−Gpp(NH)p−Met-tRNA$_i^{Met}$ complexes were measured. Hence, we show that the eukaryotic γ subunit by itself is able to bind Met-tRNA$_i^{Met}$. This result is in keeping with those obtained with archaeal γ subunits (*5*, *6*) and further argues in favor of a tRNA binding mode for eukaryotic and archaeal e/aIF2 similar to that observed for EF-Tu (*5*, *8*). Notably, α and β make similar contributions to the binding affinity of tRNA for full Encc-eIF2 (Figure 4). This contrasts with archaeal and yeast a/eIF2, in which only one of the two peripheral subunits had a major role in tRNA binding.

We addressed the question of whether the species-specific effects of the α and β subunits on the affinity of the initiator tRNA originate from the N- and C-terminal extensions of these two peripheral subunits. Neither the N-terminal extension of β nor the C-terminal extension of Encc-eIF2α significantly participates in tRNA binding. Only the C-terminal extension of Encc-eIF2β contributes moderately, by a factor of 3, to tRNA affinity. Consistent with this result, it was shown earlier that the presence of the three lysine boxes in the N-terminal extension of yeast eIF2β did not influence the GTP-dependent initiator Met-tRNA$_i^{Met}$ binding by eIF2 (*31*). Therefore, the action of the peripheral subunits α and β of Encc-eIF2 in tRNA binding is mainly mediated by the core domains of α and β.

Notably, the contributions of the α and β subunits to the Met-tRNA$_i^{Met}$ binding affinity for Encc-eIF2 are not additive, indicating that these contributions are not independent. This raises the question of the mechanism by which the two peripheral subunits influence tRNA binding. An extended set of structural data has been obtained with archaeal aIF2. In particular, structures of the isolated γ subunit (*7*, *9*), of αγ (*5*) and βγ (*32*) heterodimers, and of heterotrimers (*27*, *33*) are known. α is

bound to domain II of γ by its C-terminal domain (αD3). β is mainly bound to γ through its N-terminal α1 helix even though the two other domains of β can also contact γ (*27*, *33*). At present, no structural data concerning e/aIF2 in a complex with Met-tRNA$_i^{Met}$ are available, but the position of the tRNA was modeled from the structure of EF-Tu bound to Gpp(NH)p-Mg^{2+} and aminoacylated tRNA (*10*). In this model, stabilization in an "on" conformation of the two switch regions, involved in the binding of GTP, is crucial for the shaping of the binding site for the 3′-methionylated end of tRNA. In archaea, the α subunit strongly contributes to the tRNA binding affinity for the full aIF2 heterotrimer. However, the EF-Tu-based docking model of Met-tRNA$_i^{Met}$ bound to aIF2 shows no direct contact between α and tRNA. This led to the proposal that the participation of aIF2α in tRNA affinity is indirect. One possibility would be that the aIF2α subunit helps aIF2γ to maintain the switches in the on conformation (*5*, *10*). In archaea, β has a minor role in tRNA binding. Again, the EF-Tu-based docking model does not predict direct contacts between the tRNA molecule and the β subunit. However, in the structure of aIF2$\beta\gamma$ from *Pyrococcus furiosus* [Pf-aIF2$\beta\gamma$ (*32*)] and in that of aIF2α3$\beta\gamma$ from *S. solfataricus* [Ss-aIF2α3$\beta\gamma$ (*33*)], the β subunit is in contact with γ through switch 1. Therefore, both α and β may help γ to maintain the switch on conformation via interactions between part of their core domains and γ. Following this idea, the nonadditivity of the contributions of α and β subunits to the Met-tRNA$_i^{Met}$ binding affinity is consistent with an indirect participation of both peripheral subunits in tRNA affinity. Indeed, once one subunit has exerted its role in the stabilization of the switch regions for the shaping of the tRNA binding site, the influence of the second peripheral subunit would become less important. An alternative hypothesis is that γ is partially unfolded and that binding of either peripheral subunit to it stabilizes the folded state. However, the fact that γ is well-produced, stable during purification, and able to bind tRNA in a GTP-dependent manner disfavors the idea of a global effect of α and β on the fold of γ. In addition, as noted above, the $\alpha-\gamma$ and $\beta-\gamma$ interfaces correspond to limited regions at the surface of γ. Therefore, we favor the idea of a stabilizing effect of α and β specifically directed to the switch regions.

To conclude, it can be proposed that modulation of the interactions at the interfaces between α and γ, or between β and γ, is at the origin of the species-specific distribution of the roles of the peripheral subunits of e/aIF2 in tRNA binding. The sequence alignments in this study failed to identify obvious differences in residues involved in the interfaces between subunits. Therefore, subtle adjustments at these interfaces may be at the origin of the different behaviors of the studied e/aIF2 factors.

ACKNOWLEDGMENT

We thank Pr. F. Delbac (UMR CNRS 6023 Laboratoire Microorganismes, Génome et Environnement, 63177 Aubière Cedex, France) for the generous gift of *E. cuniculi* DNA. We thank Thomas Simonson for critical reading of the manuscript.

SUPPORTING INFORMATION AVAILABLE

Alignments of e/aIF2α sequences (Figure S1), e/aIF2β sequences (Figure S2), and e/aIF2γ sequences (Figure S3). This material is available free of charge via the Internet at http://pubs.acs.org.

REFERENCES

1. Lorsch, J., and Dever, T. (2010) Molecular view of 43S complex formation and start site selection in eukaryotic translation initiation. *J. Biol. Chem. 285*, 21203–21207.
2. Erickson, F. L., and Hannig, E. M. (1996) Ligand interactions with eukaryotic translation initiation factor 2: Role of the γ-subunit. *EMBO J. 15*, 6311–6320.
3. Kapp, L. D., and Lorsch, J. R. (2004) GTP-dependent Recognition of the Methionine Moiety on Initiator tRNA by Translation Factor eIF2. *J. Mol. Biol. 335*, 923–936.
4. Pedulla, N., Palermo, R., Hasenohrl, D., Blasi, U., Cammarano, P., and Londei, P. (2005) The archaeal eIF2 homologue: Functional properties of an ancient translation initiation factor. *Nucleic Acids Res. 33*, 1804–1812.
5. Yatime, L., Mechulam, Y., Blanquet, S., and Schmitt, E. (2006) Structural switch of the γ subunit in an archaeal aIF2$\alpha\gamma$ heterodimer. *Structure 14*, 119–128.
6. Yatime, L., Schmitt, E., Blanquet, S., and Mechulam, Y. (2004) Functional molecular mapping of archaeal translation initiation factor 2. *J. Biol. Chem. 279*, 15984–15993.
7. Schmitt, E., Blanquet, S., and Mechulam, Y. (2002) The large subunit of initiation factor aIF2 is a close structural homologue of elongation factors. *EMBO J. 21*, 1821–1832.
8. Nissen, P., Kjeldgaard, M., Thirup, S., Polekhina, G., Reshetnikova, L., Clark, B. F. C., and Nyborg, J. (1995) Crystal structure of the ternary complex of Phe-tRNA^{Phe}, EF-Tu, and a GTP analog. *Science 270*, 1464–1472.
9. Roll-Mecak, A., Alone, P., Cao, C., Dever, T. E., and Burley, S. K. (2004) X-ray structure of translation initiation factor eIF2γ: Implications for tRNA and eIF2α binding. *J. Biol. Chem. 279*, 10634–10642.
10. Schmitt, E., Naveau, M., and Mechulam, Y. (2010) Eukaryotic and archaeal translation initiation factor 2: A heterotrimeric tRNA carrier. *FEBS Lett. 584*, 405–412.
11. Nika, J., Rippel, S., and Hannig, E. M. (2001) Biochemical analysis of the eIF2$\beta\gamma$ complex reveals a structural function for eIF2α in catalyzed nucleotide exchange. *J. Biol. Chem. 276*, 1051–1060.
12. Flynn, A., Oldfield, S., and Proud, C. G. (1993) The role of the β-subunit of initiation factor eIF-2 in initiation complex formation. *Biochim. Biophys. Acta 1174*, 117–121.
13. Katinka, M. D., Duprat, S., Cornillot, E., Metenier, G., Thomarat, F., Prensier, G., Barbe, V., Peyretaillade, E., Brottier, P., Wincker, P., Delbac, F., El Alaoui, H., Peyret, P., Saurin, W., Gouy, M., Weissenbach, J., and Vivares, C. P. (2001) Genome sequence and gene compaction of the eukaryote parasite *Encephalitozoon cuniculi*. *Nature 414*, 450–453.
14. Thomarat, F., Vivares, C. P., and Gouy, M. (2004) Phylogenetic analysis of the complete genome sequence of *Encephalitozoon cuniculi* supports the fungal origin of microsporidia and reveals a high frequency of fast-evolving genes. *J. Mol. Evol. 59*, 780–791.
15. Keeling, P. J. (2003) Congruent evidence from α-tubulin and β-tubulin gene phylogenies for a zygomycete origin of microsporidia. *Fungal Genet. Biol. 38*, 298–309.
16. Tanabe, Y., Watanabe, M., and Sugiyama, J. (2002) Are microsporidia related to fungi? A reappraisal based on additional gene sequences from basal fungi. *Mycol. Res. 106*, 1380–1391.
17. Guillon, L., Schmitt, E., Blanquet, S., and Mechulam, Y. (2005) Initiator tRNA binding by e/aIF5B, the eukaryotic/archaeal homologue of bacterial initiation factor IF2. *Biochemistry 44*, 15594–15601.
18. Guillon, J. M., Meinnel, T., Mechulam, Y., Lazennec, C., Blanquet, S., and Fayat, S. (1992) Nucleotides of tRNA governing the specificity of *Escherichia coli* methionyl-tRNA$^{Met}_f$ formyltransferase. *J. Mol. Biol. 224*, 359–367.
19. Meinnel, T., and Blanquet, S. (1995) Maturation of pre-tRNA^{fMet} by *E. coli* RNase P is specified by a guanosine of the 5′ flanking sequence. *J. Biol. Chem. 270*, 15906–15914.
20. Meinnel, T., Mechulam, Y., and Fayat, G. (1988) Fast purification of a functional elongator tRNA^{Met} expressed from a synthetic gene *in vivo*. *Nucleic Acids Res. 16*, 8095–8096.
21. Mellot, P., Mechulam, Y., LeCorre, D., Blanquet, S., and Fayat, G. (1989) Identification of an amino acid region supporting specific methionyl-tRNA synthetase:tRNA recognition. *J. Mol. Biol. 208*, 429–443.
22. Brevet, A., Chen, J., Lévêque, F., Plateau, P., and Blanquet, S. (1989) *In vivo* synthesis of adenylated bis(5′-nucleosidyl) tetraphosphates (Ap_4N) by *Escherichia coli* aminoacyl-tRNA synthetases. *Proc. Natl. Acad. Sci. U.S.A. 86*, 8275–8279.
23. Mechulam, Y., Guillon, L., Yatime, L., Blanquet, S., and Schmitt, E. (2007) Protection-based assays to measure aminoacyl-tRNA binding to translation initiation factors. *Methods Enzymol. 430*, 265–281.

24. Dardel, F. (1994) MC-Fit: Using Monte-Carlo methods to get accurate confidence limits on enzyme parameters. *CABIOS, Comput. Appl. Biosci. 10*, 273–275.
25. Thompson, G. M., Pacheco, E., Melo, E. O., and Castilho, B. A. (2000) Conserved sequences in the β subunit of archaeal and eukaryal translation initiation factor 2 (eIF2), absent from eIF5, mediate interaction with eIF2γ. *Biochem. J. 347*, 703–709.
26. Hashimoto, N. N., Carnevalli, L. S., and Castilho, B. A. (2002) Translation initiation at non-AUG codons mediated by weakened association of eukaryotic initiation factor (eIF) 2 subunits. *Biochem. J. 367*, 359–368.
27. Stolboushkina, E., Nikonov, S., Nikulin, A., Blasi, U., Manstein, D. J., Fedorov, R., Garber, M., and Nikonov, O. (2008) Crystal structure of the intact archaeal translation initiation factor 2 demonstrates very high conformational flexibility in the α- and β-subunits. *J. Mol. Biol. 382*, 680–691.
28. Marck, C., and Grosjean, H. (2002) tRNomics: Analysis of tRNA genes from 50 genomes of Eukarya, Archaea, and Bacteria reveals anticodon-sparing strategies and domain-specific features. *RNA 8*, 1189–1232.
29. Schulman, L. H., and Pelka, H. (1988) Anticodon switching changes the identity of methionine and valine transfer RNAs. *Science 242*, 765–768.
30. Hannig, E. M., Cigan, A. M., Freeman, B. A., and Kinzy, T. G. (1993) GCD11, a negative regulator of GCN4 expression, encodes the γ subunit of eIF-2 in *Saccharomyces cerevisiae*. *Mol. Cell. Biol. 13*, 506–520.
31. Laurino, J. P., Thompson, G. M., Pacheco, E., and Castilho, B. A. (1999) The β subunit of eukaryotic translation initiation factor 2 binds mRNA through the lysine repeats and a region comprising the C2-C2 motif. *Mol. Cell. Biol. 19*, 173–181.
32. Sokabe, M., Yao, M., Sakai, N., Toya, S., and Tanaka, I. (2006) Structure of archaeal translational initiation factor 2 $\beta\gamma$-GDP reveals significant conformational change of the β-subunit and switch 1 region. *Proc. Natl. Acad. Sci. U.S.A. 103*, 13016–13021.
33. Yatime, L., Mechulam, Y., Blanquet, S., and Schmitt, E. (2007) Structure of an archaeal heterotrimeric initiation factor 2 reveals a nucleotide state between the GTP and the GDP states. *Proc. Natl. Acad. Sci. U.S.A. 104*, 18445–18450.